Ultrasound assisted crystallization of a new cardioactive prototype using ionic liquid as solvent

Jacqueline Resende de Azevedo, Fabienne Espitalier, Maria-Inês Ré

Ultrasound assisted crystallization of a new cardioactive prototype using ionic liquid as solvent

Jacqueline Resende de Azevedo[a,b], Fabienne Espitalier[a,*], Maria Inês Ré[a]

[a] Université de Toulouse, Mines-Albi, UMR-CNRS 5302, Centre RAPSODEE, Campus Jarlard, F-81013 Albi CT cedex 09, France
[b] Univ Lyon, Université Claude Bernard Lyon 1, CNRS, LAGEPP UMR 5007, 43 boulevard du 11 novembre 1918, F-69100 Villeurbanne, France[1]

A B S T R A C T

This work deals with the antisolvent crystallization of LASSBio-294 (3,4-methylenedioxybenzoyl-2-thienylhydrazon) assisted by ultrasound. An ionic liquid (IL), 1-ethyl-3-methylimidazolium methyl phosphonate [emim][$CH_3O(H)PO_2$] was used as solvent and water as antisolvent. The influence of the following parameters on crystals properties (size distribution, morphology, residual solvent and *in vitro* dissolution) were studied with two mixing mode (quick and dropwise) of solution with antisolvent. The impact of washing and drying process was also evaluated. Comparative studies of conventional crystallization conditions (without ultrasound) were also performed. The effect of ultrasound on LASSBio-294 recrystallized properties was influenced by the add mode, water/IL ratio and drug solution concentration. As example, US promoted the formation of small crystals with high residual IL under the following conditions: quick addition, high drug solution concentration and high water/IL ratio. However, despite the decrease of elementary particle size, ultrasound did not avoid crystals agglomeration. The drug dissolution rate was affected by the physical structure of agglomerates. When employed as drying process of washed crystals, spray drying reduced this agglomeration and improved the dissolution of LASSBio-294 crystals.

Keywords:
Poorly water-soluble drug
Ionic liquid
Ultrasound
Crystallization

1. Introduction

LASSBio-294, 3,4-Methylenedioxybenzoyl-2-thienylhydrazone is a drug candidate for the treatment of cardiac failure and prevention of myocardial infarction induced by cardiac dysfunction [1,2]. Since LASSBio-294 integrates the category of the poorly water-soluble drugs, its bioavailability could be limited.

Poor aqueous solubility of a drug entity can be addressed with various pharmaceutical particle technologies, among them, the modification of drug crystal properties like reduction of particle size within microscale or to nanoscale [3].

Antisolvent crystallization is an effective way to prepare micro or nano-sized drug particles. The technique involves the mixing of two miscible fluids: the drug dissolved in a solvent and an antisolvent, which reduces the drug solubility in the solvent, causing the drug to crystallize out of the solution. The mixing generates high supersaturation that favors nucleation and then the formation of small crystal. The properties of the final crystalline product such as size, morphology and purity are significantly dependent on the rate, magnitude and uniformity of the supersaturation generated during this process [4]. Poor mixing between drug solution and antisolvent leads to accidental zones of supersaturation, heterogeneous growth of crystals affecting the particle size and morphological features.

One technical requirement associated with this crystallization technique is a reasonable solubility of the drug in the solvent. A large part of pipeline drug entities lacks sufficient solubility in organic solvents typically used for recrystallization, as ethanol. To overcome this problem, supercritical fluids and ionic liquids are some of the alternative solvents which have been currently tested as good solvents for drugs poorly soluble in traditional volatile organic solvents [5].

Ionic liquids (IL) are defined as salts composed of separate cations and anions with melting points below 100 °C. In general, they are thermally stable, nonflammable and exhibit very low vapor pressure. The particular use of ILs as solvents for pharmaceutical drugs has been described [6–11]. Few studies in the literature deals with the use of ILs as solvents for drug crystallization purposes [11–14] and different effects on the final products were reported, for instance, the production of ultrafine amorphous particles of rifampicin [15] or the obtention of

* Corresponding author.
E-mail addresses: jacqueline.resende-de-azevedo@univ-lyon1.fr (J. Resende de Azevedo), fabienne.espitalier@mines-albi.fr (F. Espitalier), maria-ines.re@mines-albi.fr (M.I. Ré).
[1] Current address.

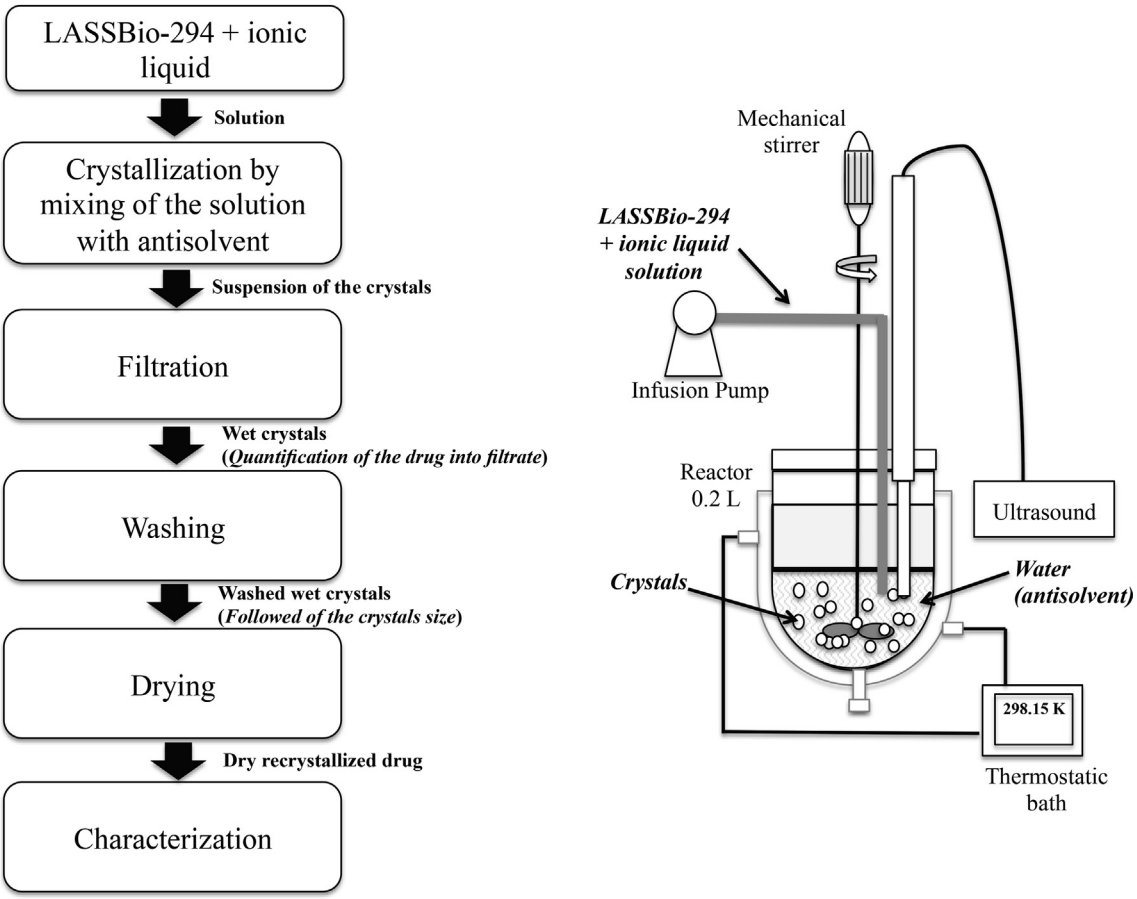

Fig. 1. Experimental set-up and process steps for LASSBio-294 antisolvent crystallization studies.

new polymorphs of adefovir dipivoxil [16,17].

Our group has previously reported promising results of solubility of LASSBio-294 in seven imidazolium based ionic liquids miscible or partially miscible with water (1-ethyl-3-methylimidazolium methyl phosphonate [emim][$CH_3(H)PO_2$, 1-ethyl-3-methylimidazolium ethyl phosphonate [emim][$CH_3CH_2O(H)PO_2$], 1-ethyl-3-methylimidazolium acetate [emim][CH_3OO], 1,3-dimethylimidazolium methyl phosphonate [dmim][$CH_3O(H)PO_2$], 1-butyl-3-methylimidazolium acetate [bmim][CH_3OO], 1-butyl-3-methylimidazolium tetrafluoroborate [bmim][BF_4] and 1-butyl-3-methylimidazolium bis(trifluoromethanesulfonyl)imide [bmim][NTf_2] [18]. Interactions such as hydrogen bonds, van der Waals forces and π-π-solvent-solvent interactions permitted to explain the difference of solubility observed.

In addition LASSBio-294 antisolvent crystallization was performed using 1-ethyl-3-methylimidazolium methyl phosphonate [emim][$CH_3(H)PO_2$] as solvent and water as antisolvent was performed [12,19]. In this study, pre-mixer was used to mix the drug/solvent solution and the anti-solvent. The results revealed that the intense mixing promote with pre-mixers at high solute concentration (159 $mg \cdot g^{-1}$ solution) seemed to favor the formation of smaller crystals more than without pre-mixer. However, the formation of a gel phase was observed in some operating conditions. Nevertheless, the amount of residual solvent was lower without pre-mixer allowing a better definition of crystals edges.

In the present study, the crystallization was conducted in a stirred vessel without pre-mixer in order to minimize the residual ionic liquid in crystals. Application of ultrasound is known to provide uniform mixing conditions throughout the vessel during antisolvent process. Indeed, ultrasound intensifies the mass transfer when it propagates through a liquid medium due to the formation of cavitation bubbles. These effects bring considerable benefits to crystallization processes, such as rapid induction of primary nucleation, reduction of crystal size, inhibition of agglomeration and manipulation of crystal size distribution [20]. Reports about ILs-based processes assisted by ultrasound have been described for synthesis of Bi_2S_3 nanoparticles [21], quinolines [22] and imidazolium salts [23]. These studies have motivated the investigation of the ultrasound effect during LASSBio-294 crystallization. The influence of the following parameters on crystals properties (size distribution, morphology, residual solvent and *in vitro* dissolution) was investigated: the add mode (quick and dropwise) of the solution into the vessel, the LASSBio-294 concentration in the solution, the water/IL mass ratio and the ultrasound power. The effect of washing and drying methods was also evaluated. Experiments without ultrasound was conducted for comparison.

2. Experimental section

2.1. Materials

The LASSBio-294 was obtained from Cristália Ltda (Itapira, SP, Brazil) and used without further purification. It is in the form of a yellowish solid with a molecular weight of 274.3 $g \cdot mol^{-1}$ and 99.96% wt purity. The ionic liquid, 1-ethyl-3-methylimidazolium methyl phosphonate ([emim][$CH_3O(H)PO_2$]), was obtained from Solvionic (Toulouse, France) and it was used as received (> 98% pure). Sodium dodecyl sulfate (SDS) was supplied by VWR International (Leuven, Belgium) for *in vitro* dissolution. HPLC grade acetonitrile (Scharlau SL, Spain), methane sulfonic acid (MSA) (Fluka, Buchs, Switzerland) for ion chromatography were used to prepare the mobile phases. Sodium dihydrogen phosphate (NaH_2PO_4) (Sigma-Aldrich, Gillingham-Dorset, England) and sodium hydrogen phosphate (Na_2HPO_4) (Alfa Aesar, Karlsruhe, Germany) of analytical grade were used to prepare the

buffers and mobile phases. Water was distilled and purified using Milli-Q Water Purification System (Purelab Classic DI MK2, Elga, UK).

2.2. Crystallization method

LASSBio-294 solution at defined concentration (29, 57 or 159 mg·g^{-1} solution) was prepared in [emim][$CH_3O(H)PO_2$] as solvent at 303.15 ± 0.5 K. The antisolvent (water) was introduced into a 0.2 L glass vessel (diameter 6.3 cm) with double jacket equipped with a mechanical turbine stirrer with 8 blades mounted on flat disc throughout the operation. The temperature at 298.15 ± 0.5 K was controlled by a water bath (Julabo VC F30). Agitation at 800 rpm was powered using a mechanical stirrer (Eurostar IKA labortechnick 2000 motor). Based on preliminary tests and solid-liquid equilibrium of our ternary system, mass ratios water/[emim][$CH_3O(H)PO_2$] between 3.7 and 14.9 were used [19]. These mass ratios permit to maximize the crystals yield. Two modes for mixing drug solution and antisolvent were employed: quick (injection time equal to 50 s) and dropwise (injection time between 20 and 22 min) using an infusion pump (Harvard PHD 2000 Infusion, USA). Ultrasound (SINAPTEC, Lezennes, France) was used during the solution addition. The frequency of ultrasound was 20 kHz and dissipated power was ranged between 10 and 40 W (Fig. 1). As soon addition was over the suspension was stirred for 30 min at atmospheric pressure and 298.15 K then filtered (pore size 0.2 µm, polypropylene, Millipore, Bedford, MA, UK), and washed with water (500 g, method 1) to remove the residual solvent. The particle size distribution of the washed solids was measured by laser granulometry. Crystals were then dried in vacuum oven (Heraeus Vacutherm-VT-6025) at 323.15 K for 3–5 days and then further characterized (size, crystalline structure, morphology, residual solvent and *in vitro* dissolution). All experimental conditions are given in Table 1.

2.3. Optimization of the washing process

In order to reduce the crystals residual solvent, two new washing methods were tested (methods 2 and 3) with products of experiment 5. In both cases, washing was performed in four steps with 1000 g of water, doubling its amount from the method 1. In method 2, 250 g of water were added directly into the filtration system and mixed with the crystals. Once the filtration was finished, 250 g of water were added again, then twice more. In method 3, each mixture of wet crystals with water (250 g) was kept under magnetic stirring for 10 min before filtration process.

2.4. Optimization of the drying process

To reduce observed crystals agglomeration during drying in oven, spray drying was applied as an alternative drying method. Four additional experiments were then performed as replicates of experiments 5 and 9 (with ultrasound) and 6 and 10 (without ultrasound). After the washing process, the crystals obtained were re-dispersed in pure water. The new aqueous dispersions were then spray-dried with a 0.7 mm two-fluid pressurized atomizer at a feed rate of 2 g·min^{-1} in a laboratory-scale mini spray dryer (Büchi Mini Spray-dryer B-290, Switzerland). The atomizing air flow rate was 500–600 NL·h^{-1}. The inlet temperature was controlled at 383.15 ± 5 K and the outlet temperature (363.15 ± 5 K) was determined by the inlet temperature and relative factors such as air and liquid flow rates.

2.5. Characterization

2.5.1. Particle size

Mean particle size and particle size distribution were determined by laser diffraction using a Mastersizer 3000 (Malvern Instruments. UK). Raw LASSBio-294 and recrystallized samples (washed wet and dry crystals) were adequately dispersed in distilled water before each measurement. A few drops of suspension were added directly into the tank of the laser diffractometry containing water until the desired range (5–15%) of laser obscuration level was reached. A refractive index of 1.520 was used for the particles (by default use) and 1.33 for the continuous phase (water). The samples circulated in the measuring cell using the instrument's internal stirring system (2200 rpm). Results were expressed as number or volume percentage (%) according to the particle size diameter (µm). The mean surface diameter, $D_{3,2}$, and mean volume diameter, $D_{4,3}$, calculations were done by using the Malvern 3000 software version 3.20 supplied by the manufacturer (Malvern Instruments Ltd.).

2.5.2. Scanning electron microscopy (SEM)

The morphology of powder samples was visualized using an Environmental Scanning Electron Microscope-Field Emission Gun microscope (Philips XL30 FEG, ESEM-FEG, FEI Company). The samples were fixed on an SEM stub using double-sided adhesive tape and coated with platinum using a Polaron SC7640 high resolution SEM sputter coater (Quorom Technologies, England). Images were taken with an accelerating voltage of 20 kV.

Table 1
Summary of experimental conditions and results of the characterization of products.

Experiment number	Concentration (mg·g^{-1} solution)	Water/IL ratio	Power of ultrasound (W)	S*	$D_{4,3}$ (µm)	$D_{3,2}$ (µm)	Residualsolvent (ppm)
Quick addition							
1	159	13.9	0	14,918	14.0	3.0	6920
2	159	14.9	40	14,687	0.6	0.5	29,904
3	159	3.7	0	9099	2.6	0.8	12,055
4	159	3.9	40	9470	10.8	2.0	45,674
5	57	4.7	0	3715	4.0	1.3	18,240
6	57	4.7	40	3680	4.0	1.2	1176
Dropwise addition							
7	57	13.3	0	4859	7.0	2.0	984
8	57	13.1	40	4871	1.8	0.8	933
9	57	4.6	0	3640	7.4	2.5	1265
10	57	4.6	40	3633	2.4	1.1	956
11	159	4.5	40	11,011	2.3	1.3	13,273
12	29	4.7	40	1851	2.3	1.1	887
13	57	4.6	30	3636	1.7	0.8	904
14	57	4.9	20	3918	1.8	0.9	1414
15	57	4.7	10	3678	6.8	2.7	9517

* Maximal supersaturation ratio = Ci/Ceq.

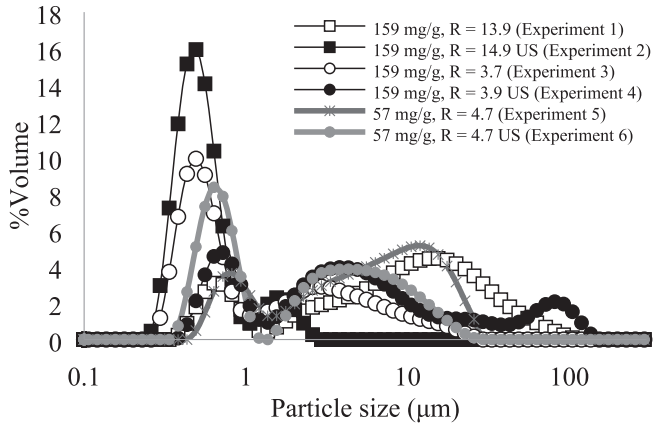

Fig. 2. Particle size distribution of recrystallized LASSBio-294 by quick addition.

2.5.3. X-ray diffractometry (XRD)

The samples were analysed by XRD diffractometry (Philips X'Pert diffractometer, PanAlytical, USA). The measurements were performed using CuKα radiation at a scanning rate of 0.018° min^{-1} from 8 to 40°, applying 45 kV and 40 mA. The diffraction patterns were collected in an angular range of 10–35°-2θ.

2.5.4. Specific surface area

The specific surface area was measured in a Surface Area Analyzer and Porosity Analyser (Tristar II 3020, Micromeritics Instruments Co., USA) using the nitrogen adsorption method. In this method, calculation was based on the BET equation. Before measuring, the sample powders were degassed.

2.5.5. Residual solvent

A Dionex model ICS-3000 ion chromatograph was applied to determine the residual solvent amount in the crystals by the quantification of cation-IL. This system consists of an autosampler, a degasser, pumps and conductometric detector. A Dionex suppressor LERS 500 (4 mm) for chemical suppression was installed between the conductometric detector and the Dionex IonPac CS17 analytical column (250 mm × 4 mm). A Dionex IonPac CG17 (50 mm × 4 mm) guard column was also installed. The samples were eluted by isocratic elution with acetonitrile-MSA 20 mM mixtures (20:80 (w/w)) at a flow rate of 1.0 mL·min^{-1}. An injection volume of 25 µL was used. All chromatographic analyses were carried at 308.15 ± 0.5 K. Cation-IL concentration in the crystals was determined from solutions prepared with 100% acetonitrile. The concentrations were calculated with linear regression equation (Peak area (µS·min) = 0.0165C (µg·g^{-1} solution) − 0.0495, R^2 = 0.9954) obtained with the linear ranges of calibration curve between peak area and the concentration (0.6–144 µg·g^{-1} solution).

2.5.6. Dissolution test

Dissolution studies were performed using an Erweka DT60 dissolution apparatus (Erweka, Germany), according to the paddle method (USP) and under sink-conditions (maximal concentration 15 µg/mL, which is, lower than the third of the equilibrium concentration). The stirring speed used was 50 rpm, and the temperature was maintained at 310.15 K ± 0.5 K (n = 3). The dissolution medium (900 g) was phosphate buffer pH 7.4 containing SDS 0.5%. The phosphate buffer consisted of a mixture 1.2% sodium dihydrogen phosphate (NaH_2PO_4) and 8.8% sodium hydrogen phosphate (Na_2HPO_4). Samples were taken at appropriate time intervals. Samples were filtered through a 0.2 µm filter (Acrodisc GHP, Millipore, Bedford, MA, UK) and analyzed by HPLC. The HPLC analyses were carried with a system consisted of an Agilent chromatograph (Model 1100 series) equipped with a UV–Vis detector. A reversed phase analytical Symmetry® C18 column, 100 Å, 5 µm (4.6 mm × 250 mm, WAT054275, Waters) was maintained at room temperature and equilibrated with the analytical mobile phase before injection. The mobile phase consisted of a mixture of 20% acetonitrile and 80% phosphate buffer (0.02 mol NaH_2PO_4/L with phosphoric acid 1%, pH 4.5). The flow rate was 1.0 µm^3·min^{-1}, the elution was monitored at 318 nm, and the injection volume was 0.02 cm^3. The concentrations were calculated from a linear regression equation (Peak area (mAU·s) = 61.971C (µg·g^{-1} solution) − 15.129, R^2 = 0.9990) within the linear range of the calibration curve (0.6–81 µg·g^{-1} solution). The percentage of the dissolved drug for a given time was calculated from the ratio between LASSBio-294 dissolved mass and LASSBio-294 initial mass.

3. Results and discussion

3.1. Effect of ultrasound on crystallization by quick addition

Table 1 summarizes all experimental conditions of crystallization by quick addition tests performed without (experiments 1, 3 and 5) and with ultrasound (experiments 2, 4 and 6). The influence of ultrasound was studied at high drug solution concentration (159 mg·g^{-1} solution, experiments 2 and 4) and different W/IL ratios. Experiments at low drug solution concentration and W/IL ratio was also performed (57 mg·g^{-1} solution, experiment 6). Tests in silent condition were performed for comparison.

Fig. 2 shows the particle size distributions of wet crystals obtained by quick addition. As it can be seen, with high drug solution concentration and W/IL ratio, ultrasound promoted the formation of the small crystals; the intensity of the first peak (< 1 µm) is greater. The mean volume diameter $D_{4,3}$ of the wet crystals changed from 14.1 µm in silent condition to 0.6 µm with ultrasound. At low W/IL ratio, the application of ultrasound led to particles agglomeration and increased $D_{4,3}$ of wet crystals (from 2.6 µm to 10.8 µm). This indicates that, with low W/IL ratio, smaller crystals were generated in silent conditions. In both cases, the application of ultrasound increased the residual solvent (6920 against 29904 ppm with high W/IL ratio; 12,055 against 45674 ppm with low W/IL ratio). However, with low concentration and low W/IL ratio, ultrasound favored the generation of small crystals and decreased residual solvent amounts (18240 ppm against 1176 ppm). In all cases, it could be observed that the application of ultrasound modified the morphology, making more uniform crystals with a rod-shape excepted at high W/IL ratio and high initial drug solution concentration (Fig. 3).

3.2. Effect of ultrasound on crystallization by dropwise addition

After the study with quick addition, the drug solution was introduced in the antisolvent phase by dropwise mode. With this add mode, it could be expected that each drop of organic solution may disperse more easily into the aqueous phase before the gel phase formation. Fig. 4 shows that, at the low concentration (57 mg·g^{-1} solution), independent of W/IL ratio, the presence of ultrasound led to the formation of smaller crystals (Fig. 5), with more uniform morphologies and more defined crystals edges. The same rod-shape was observed.

Whatever W/IL mass ratio, the mean volume diameter $D_{4,3}$ varied from about 7.0 (0 W) to 2.0 µm (40 W). The residual solvent decreased slightly with ultrasound, i.e., from 984 ppm to 933 ppm with high W/IL ratio and from 1265 ppm to 956 ppm with low W/IL ratio.

Experiments with ultrasound were also performed to study the influence of drug solution concentration. As shown in Fig. 6(a), the particle size distributions with 159, 57 and 29 mg·g^{-1} solution were similar in volume. The size distributions in number indicate that the intensity of the first peak (< 1 µm) is greater for the crystals prepared with 159 mg·g^{-1} solution (Fig. 6(b)). These results are confirmed by SEM images (Fig. 7). Nucleation rate is favored with a high drug

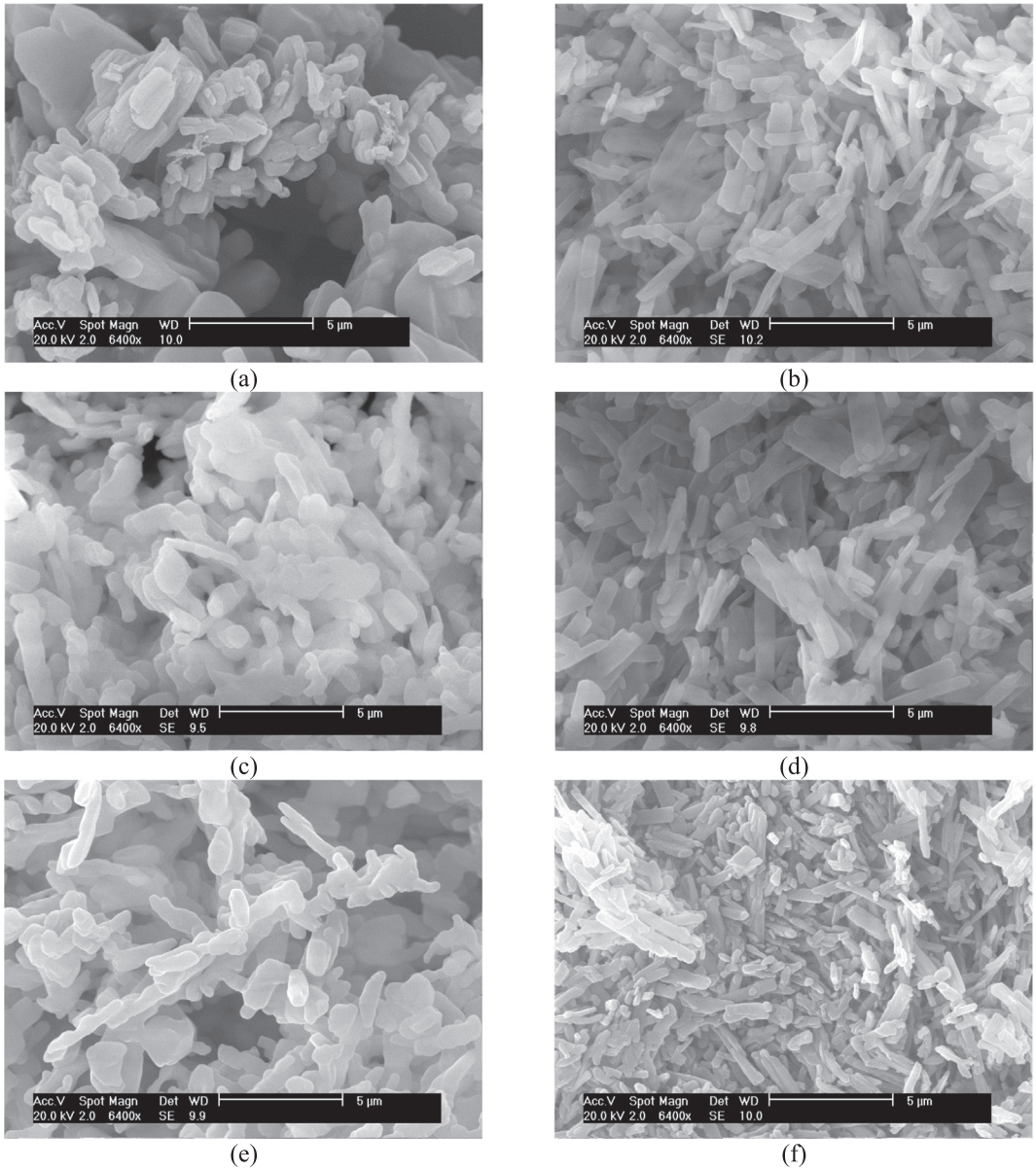

Fig. 3. SEM images of recrystallized LASSBio-294 obtained by quick addition. (a) 159 mg·g^{-1} solution and 13.9 W/IL ratio (experiment 1); (b) 159 mg·g^{-1} solution and 14.9 W/IL ratio with US (experiment 2); (c) 159 mg·g^{-1} solution and 3.7 W/IL ratio (experiment 3); (d) 159 mg·g^{-1} solution and 3.9 W/IL ratio (experiment 4); (e) 57 mg·g^{-1} solution and 4.7 W/IL ratio (experiment 5); (f) 57 mg·g^{-1} solution and 4.7 W/IL ratio with US (experiment 6).

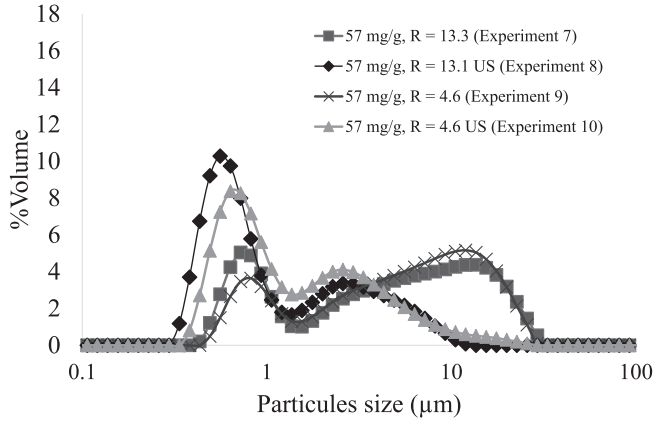

Fig. 4. Particle size distribution of recrystallized LASSBio-294 by dropwise addition.

solution concentration and smaller crystals are formed. However, solvent residual amounts increased with drug solution concentration as shown in Table 1 (887 ppm at 29 mg·g^{-1} solution, 956 ppm at 57 mg·g^{-1} solution and 13273 ppm at 159 mg·g^{-1} solution).

Some experiments were also carried to verify the influence of the ultrasound's power. The particle size distributions (Fig. 8) show that smaller crystals were generated when a power higher than 20 W is applied ($D_{4,3} \leq 2.4$ µm) (Table 1). In silent condition or with 10 W the percentage of agglomerates is higher ($D_{4,3} \geq 6.8$ µm). In silent condition or with 10 W, the percentage of agglomerates was higher ($D_{4,3} \geq 6.8$ µm). At 10 W, the cavitation bubbles seemed to induce the gelation of the system, leading to a higher residual solvent amount (9517 ppm) and less defined crystals edges, compared with results without ultrasound or with power > 20 W. The increase of power ultrasound produced more uniform crystals and no heterogeneity of crystals habit (plates and sticks) was observed at 40 W (Fig. 9).

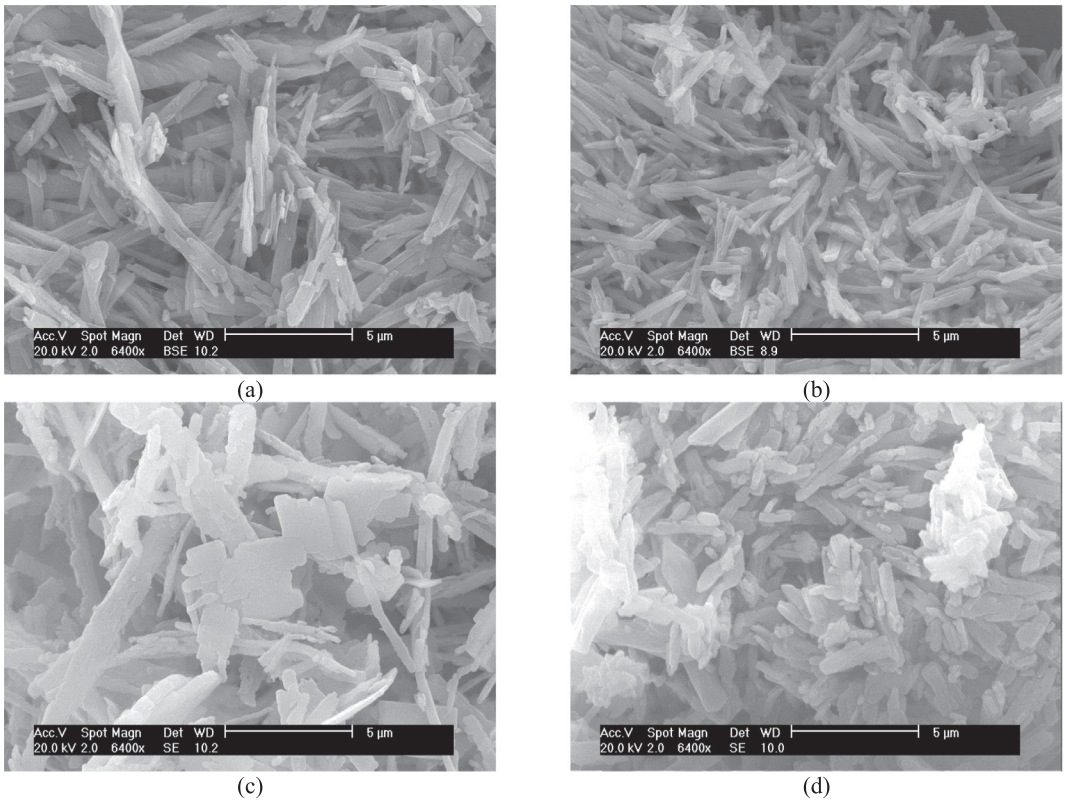

Fig. 5. SEM images of the recrystallized LASSBio-294 with low concentration (57 mg·g^{-1} solution) and dropwise injection of the solution into reactor. (a) 13.3 W/IL ratio without US; (b) 13.1 W/IL ratio with US; (c) 4.6 W/IL ratio without US and (d) 4.6 W/IL ratio with US.

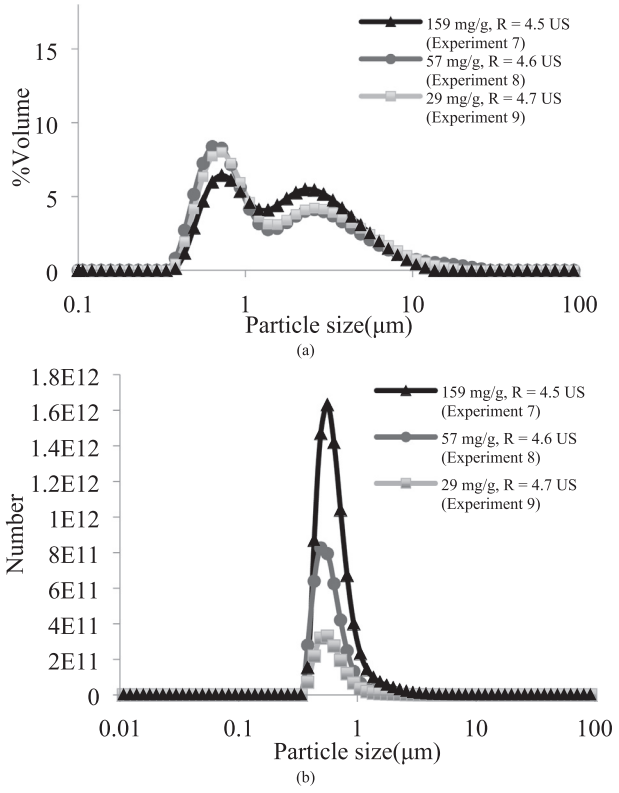

Fig. 6. Particles size distribution (a) in volume and (b) in number of recrystallized LASSBio-294 with different drug solution concentrations by dropwise addition.

3.3. Effect of crystals washing method

From solid characterization by ion chromatography, it could be confirmed that the new washing methods investigated resulted in a successful reduction of residual solvent amounts in LASSBio-294 crystals. Reductions in residual solvent from 18240 ppm (Method 1) to 2656 ppm (Method 3) and to 1503 ppm (Method 2) were detected. In methods 2 and 3, the higher water amount probably removed the "gel" formed by massive nucleation on the crystals surface. However, Fig. 10 shows that the morphologies of the crystals were modified by the different washing processes.

3.4. Effect of drying process on particle size and specific surface area (TBET) of crystals

The agglomeration of the crystals observed on the SEM images could be occurred during the synthesis in the stirred tank and/or during the drying process. The mean diameter of crystal particles dried in an oven remained almost unchanged for all experiments [12]. During drying, the "crystals agglomerates" already formed during the crystallization process are agglomerated again. Spray drying was utilized aiming to reduce this second agglomeration. Whatever the mixing mode used, the crystals dried by spray drying were smaller than those dried in an oven (Figs. 11 and 12) with decreased $D_{4,3}$ and $D_{3,2}$ values and higher specific surface area (Table 2). Compared to oven-dried crystals, the add mode (quick or dropwise) seemed to have less influence on the mean particle size of spray-dried crystals. Spray-dried crystals generated by quick addition presented higher specific surface areas.

3.5. XRD analysis

XRD analysis were performed to study the effect of the antisolvent crystallization on the crystallinity of LASSBio-294 crystals. Changes on

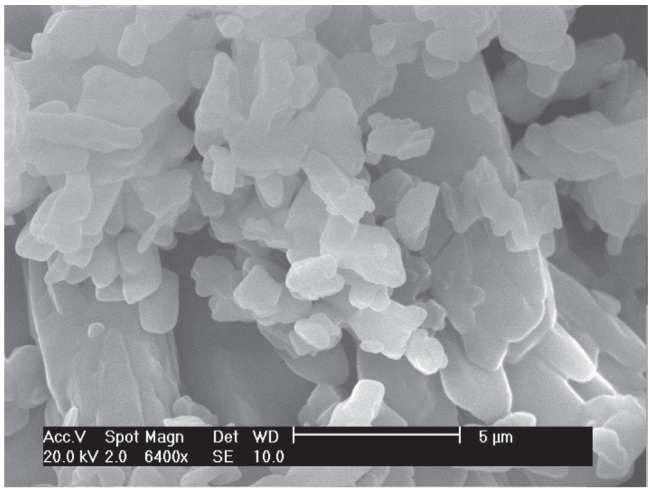

(a)

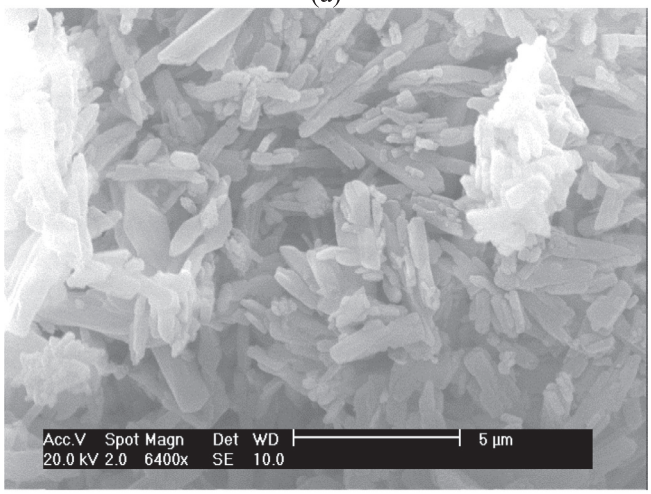

(b)

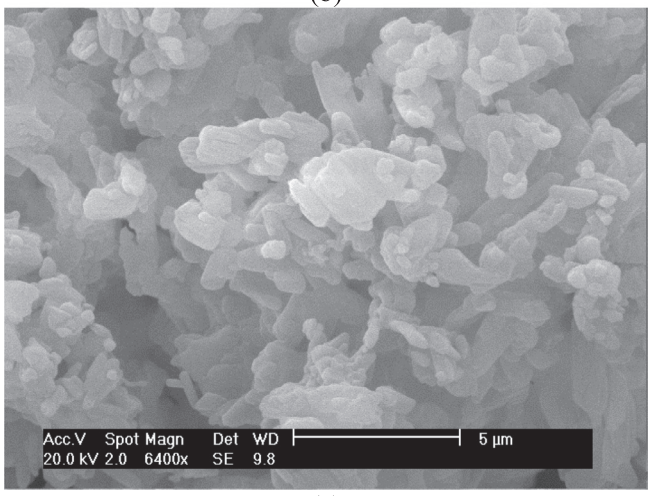

(c)

Fig. 7. SEM images of ecrystallized LASSBio-294 by dropwise injection and different concentrations: (a) 159 mg·g^{-1} solution (experiment 11), (b) 57 mg·g^{-1} solution (experiment 10) and (c) 29 mg·g^{-1} solution (experiment 12).

drug crystallinity by antisolvent crystallization has already been described [24,25]. Other studies showed that the antisolvent crystallization process using ionic liquids as solvent involved the formation of amorphous particles [15] or the development of new polymorphs [16,17]. In our study, the recrystallized LASSBio-294 exhibited the

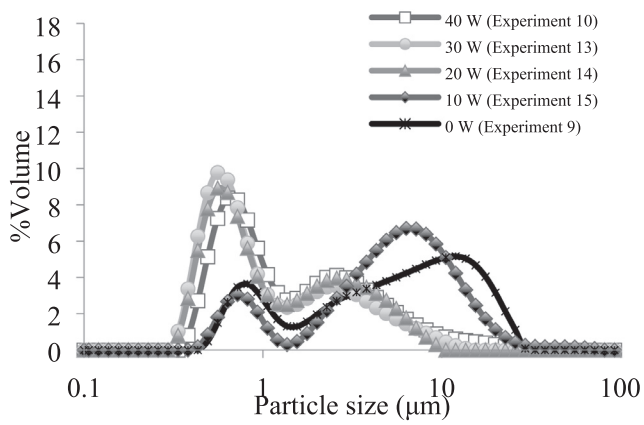

Fig. 8. Particles size distribution and SEM images of recrystallized LASSBio-294 with low concentration (57 mg·g^{-1} solution) by dropwise addition of the solution into reactor.

same crystalline peaks of the raw drug crystals (Fig. 13). However, the XRD patterns indicated changes in peaks intensities, mainly at 24.59, 25.19 and 26.54° in 2θ. This behavior is probably related to a change in the orientation and morphologies of the crystals and the reduction of the particle size.

4. Dissolution studies

4.1. Dissolution experiments

The dissolution profiles of LASSBio-294 recrystallized under different crystallization conditions and oven-dried are shown in Fig. 14. The recrystallized LASSBio-294 dissolved slower than the raw LASSBio-294. For example, after 30 min, 41% of the recrystallized drug (Experiment 9) and 75% of the original crystals are dissolved. As already discussed, LASSBio-294 is very slightly soluble in water. Its solubility in aqueous medium with SDS 0.5% increases due to the formation of surfactant micelles and micellar solubilization of the drug. Furthermore, the presence of the surfactant reduces the solid-liquid interfacial tension and increases wettability of the crystals LASSBio-294. These effects enhanced the dissolution of the LASSBio-294, explaining the higher dissolution rate of the original crystals. The results also showed that the application of ultrasound generated LASSBio-294 crystals with slower dissolution. However, when powders are examined in SEM (Fig. 15), it appears that the dissolution of recrystallized LASSBio-294 depended on both factors, crystals morphology and agglomeration/aggregation states: Dropwise without US (Experiment 9) > Quick without US (Experiment 5) > Quick with US (Experiment 6) > Dropwise with US (Experiment 10) (faster dissolution from less to more compact). No relationship was observed between the dissolution rate, residual solvent and mean size of the dry crystals. The dissolution profiles of the crystals obtained by spray drying are shown in Fig. 16. As described above, the recrystallized LASSBio-294 dissolved slower than the raw LASSBio-294. However, spray-drying crystals dissolved more rapidly than those oven-dried (Table 3). Spray drying favored the formation of smaller agglomerates, which disaggregated easier when dispersed in the dissolution medium.

4.2. Kinetic assessment and release mechanisms

The experimental kinetic dissolution profiles for recrystallized LASSBio-294 seemed to be driven by a phenomenon of diffusion limiting the crystals dissolution. Although, spray drying increased the dissolution of the crystals, diffusion probably remained the mechanism limiting the crystals dissolution. To verify this statement, the cumulative drug release from recrystallized LASSBio-294 was fitted in Higuchi

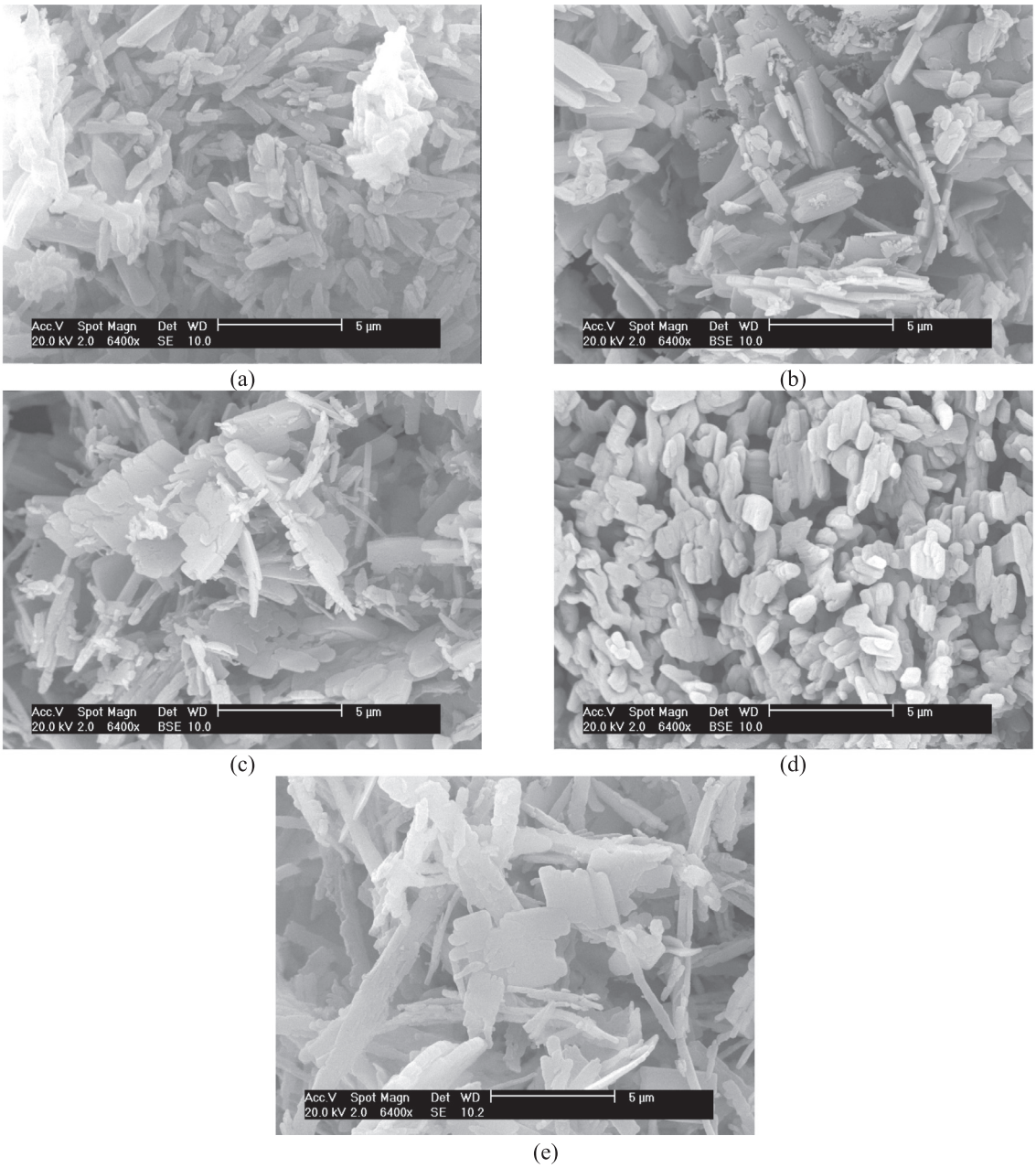

Fig. 9. SEM images of the recrystallized LASSBio-294 by dropwise addition. (a) 40 W, experiment 10); (b) 30 W, experiment 13; (c) 20 W, experiment 14; (d) 10 W, experiment 15 and (e) 0 W, experiment 9 (without ultrasound).

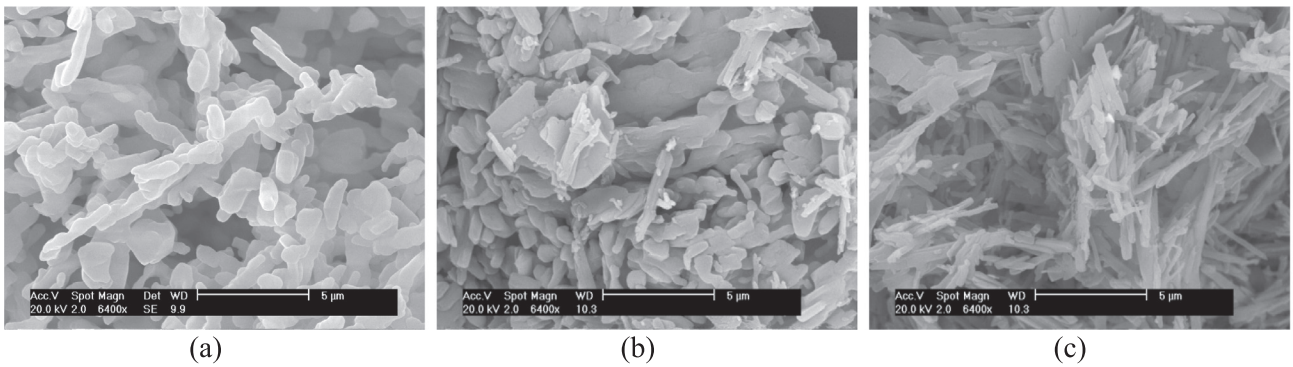

Fig. 10. SEM images of recrystallized LASSBio-294 by quick addition and different washing methods. (a) Method 1, (b) Method 2 and (c) Method 3.

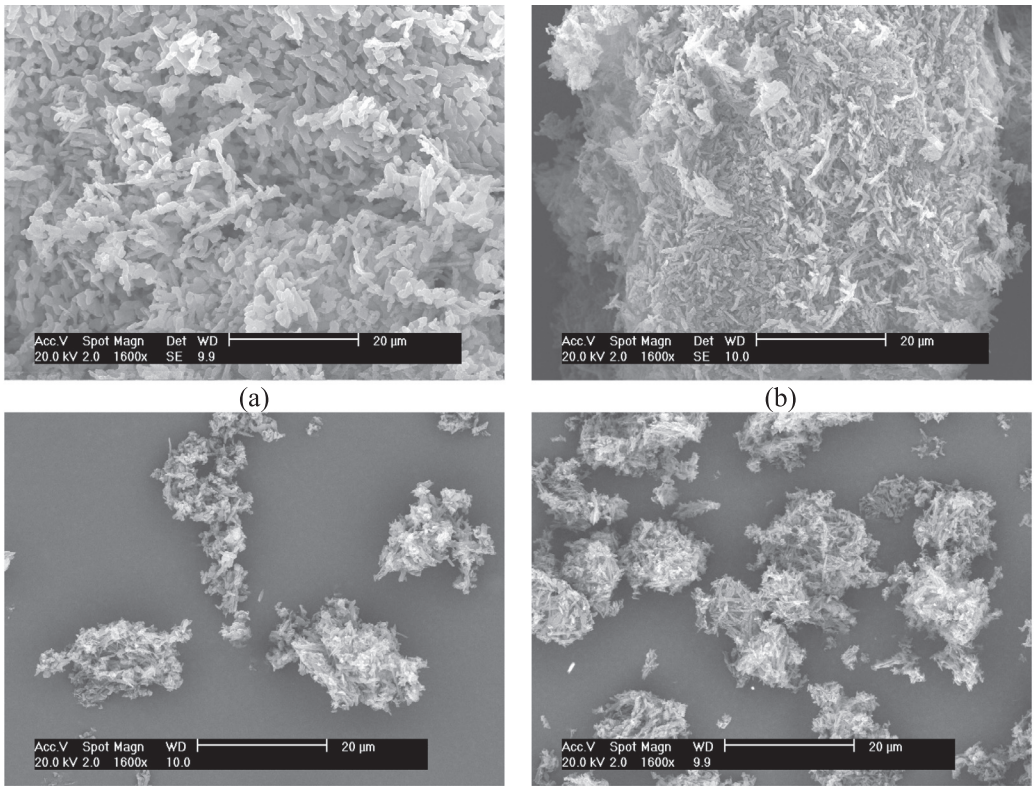

Fig. 11. SEM images of recrystallized LASSBio-294 by quick addition: effect of drying process. Oven drying: (a) without and (b) with ultrasound; Spray drying: (c) without and (d) with ultrasound.

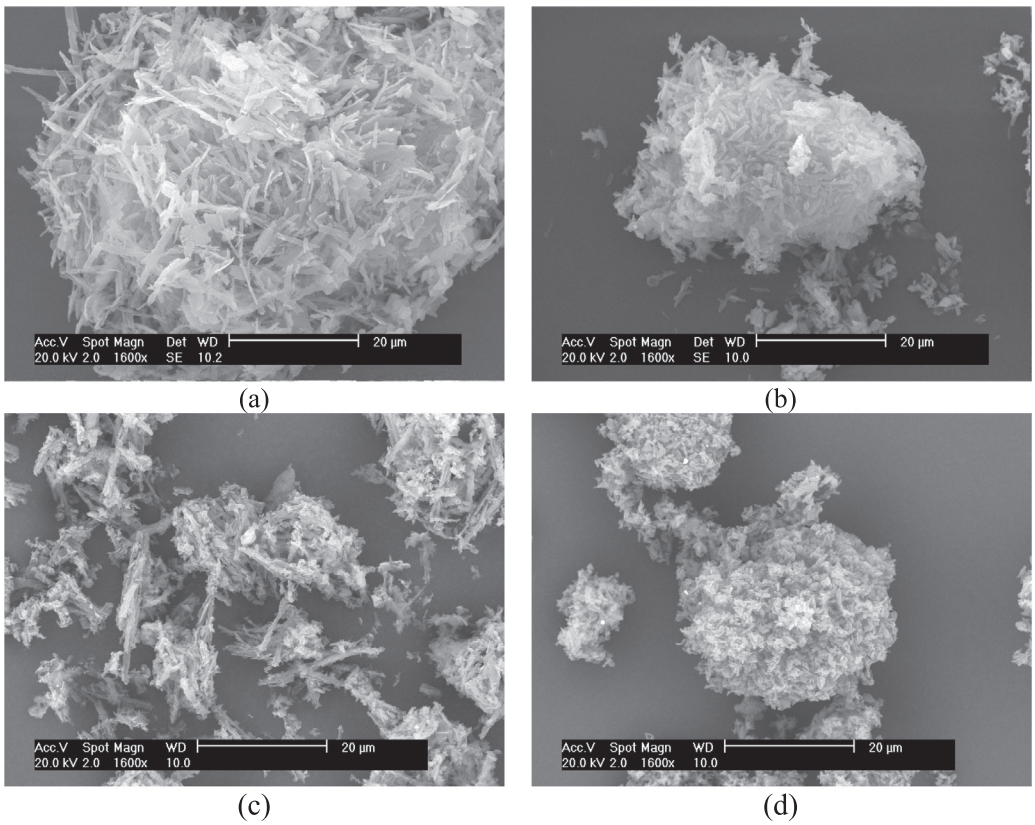

Fig. 12. SEM images of recrystallized LASSBio-294 by dropwise addition: effect of drying process. Oven drying: (a) without and (b) with ultrasound; Spray drying: (c) without and (d) with ultrasound.

Table 2
Effect of the drying method on the characteristics of LASSBio-294 crystals.

	Oven drying			Spray drying		
Addition mode	$D_{4,3}$ (μm)	$D_{3,2}$ (μm)	Specific surface ($m^2.g^{-1}$)	$D_{4,3}$ (μm)	$D_{3,2}$ (μm)	Specific surface ($m^2.g^{-1}$)
Quick, without US	6.5	2.7	1.30 ± 0.02	4.8	1.5	7.40 ± 0.09
Quick, with US	7.0	2.1	3.45 ± 0.03	4.2	1.3	7.53 ± 0.06
Dropwise, without US	9.5	3.1	1.13 ± 0.08	4.6	1.7	2.72 ± 0.14
Dropwise, with US	11.0	2.6	3.12 ± 0.03	3.6	1.4	5.78 ± 0.06

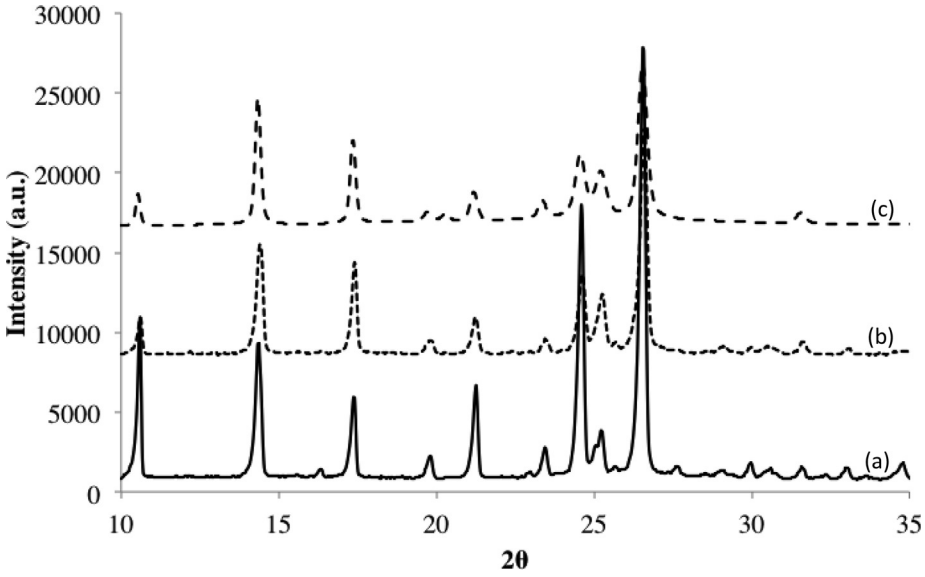

Fig. 13. XRD patterns of LASSBio-294 under different conditions. (a) raw LASSBio-294; (b) quick (experiment 5) and (c) dropwise addition (experiment 9).

model ($Q_t = K_H\sqrt{t}$), which describe the drug release from matrix system [26] and where Qt is the dissolved amount at the time, K_H is the constant Higuchi and t is the dissolution time.

The regression coefficients (R^2-values) generated following fitting of drug release data to the Higuchi model equation are summarized in Table 4, confirming that this model can well represent the dissolution mechanism of recrystallized LASSBio-294 controlled by diffusion, regardless of the crystals drying method used. Disintegration of growth units was probably related to the structure of the agglomerates. The greater agglomerates were compact, lowering diffusion of the disintegrated units. Therefore, slower is the dissolution, which implies a limited diffusion.

5. Conclusions

Antisolvent crystallization of LASSBio-294 was performed via ultrasonic process using 1-ethyl-3-methyl imidazolium methyl-phosphonate as solvent and water as antisolvent. Ultrasounds application

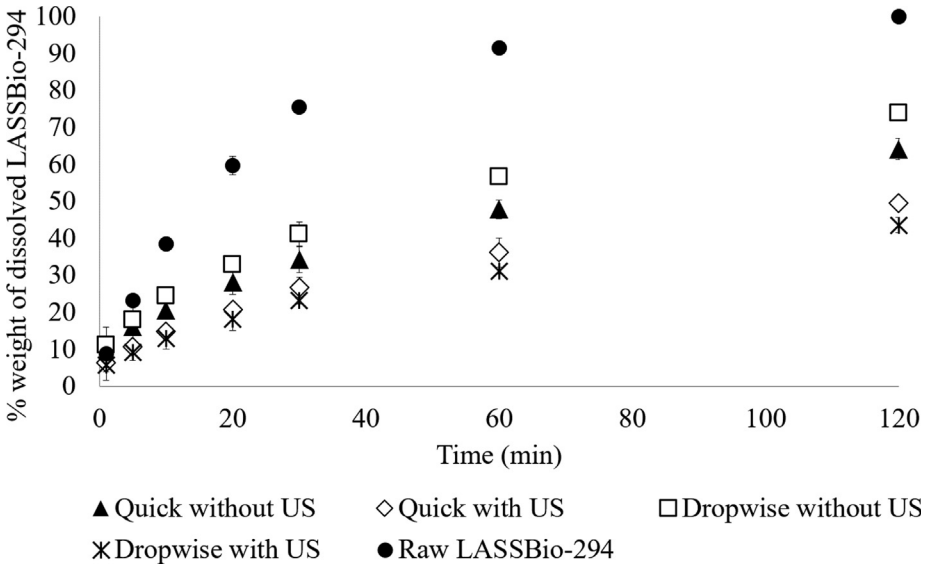

Fig. 14. Dissolution rate profiles of LASSBio-294 recrystallized under different crystallization conditions (n = 3) and oven-dried.

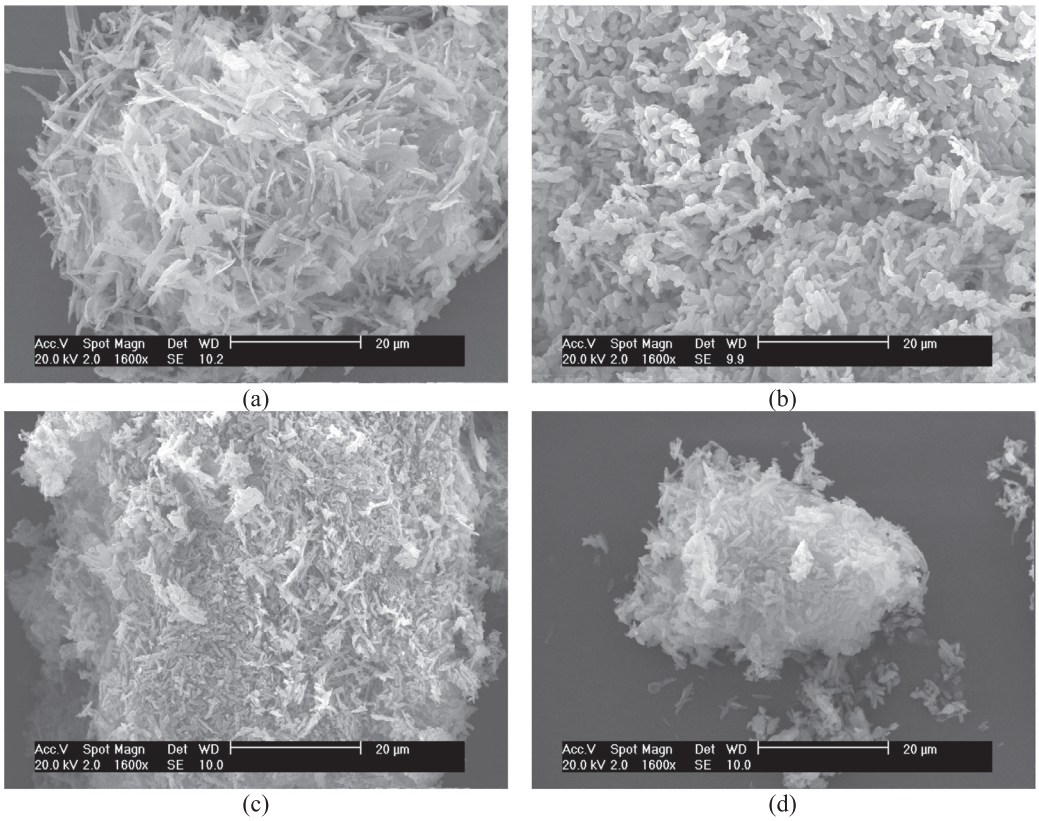

Fig. 15. SEM images of recrystallized LASSBio-294. (a) Dropwise addition without US (Experiment 9); (b) Quick addition without US (Experiment 5); (c) Quick addition with US (Experiment 6) and (d) Dropwise addition with US (Experiment 10).

allowed to modify the crystals properties and promoted the formation of the small crystals in some conditions operating, but it did not avoid crystals agglomeration. A phenomenon of "gelation" was observed at high supersaturation conditions. The system seemed to freeze and structures without defined edges and rich in residual solvent were observed. With quick addition, high drug solution concentration and W/IL ratio, smaller crystals with higher residual IL are formed compared to the conventional procedure. With dropwise addition and low drug solution concentration, regardless of W/IL ratio, the presence of ultrasound led to the formation of smaller crystals, with more uniform morphologies, more defined crystals edges and less residual IL. The dissolution rate was not enhanced by the reduction of the drug particle size, but it was affected by the physical structure of the agglomerates. Spray drying process reduced this agglomeration and improved the dissolution rate, which is controlled by diffusion (Higuchi model), regardless of the crystals drying method.

To conclude, the antisolvent crystallization method using ionic liquids as solvent can be an alternative for recrystallization of drugs poorly soluble in organic solvents, however it presents the following critical aspects that must be considered: definition of good mixing

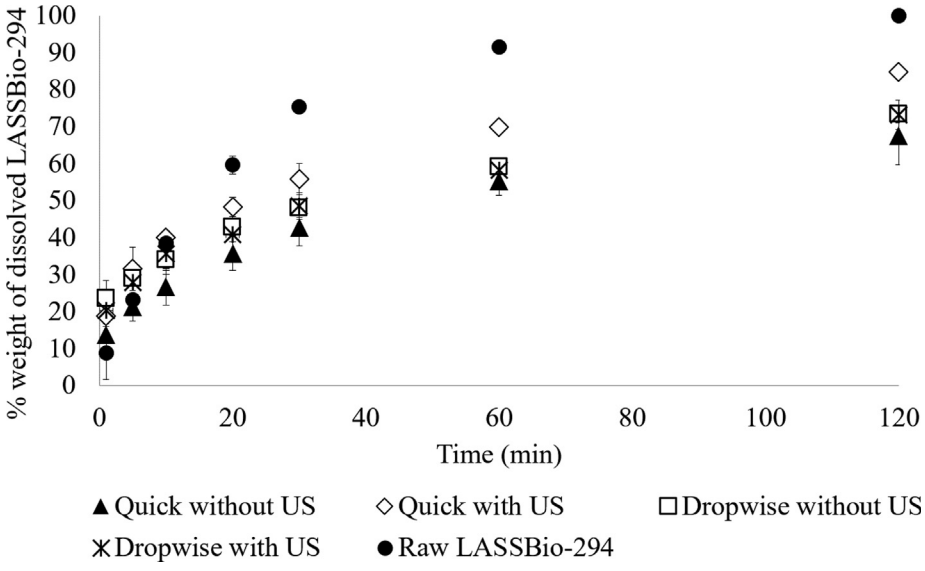

Fig. 16. Dissolution rate profiles of LASSBio-294 recrystallized under different crystallization conditions (n = 3) and dried by spray drying.

Table 3
Effect of drying process on dissolution percentage of the recrystallized LASSBio-294.

Experiment	Oven drying		Spray drying	
	Qt (%)		*Qt (%)*	
	5 min	30 min	5 min	30 min
Quick without US	16.14 ± 6.45	34.32 ± 3.52	21.24 ± 3.76	42.74 ± 4.95
Quick with US	10.66 ± 1.98	26.77 ± 2.77	31.62 ± 5.85	55.79 ± 4.23
Dropwise without US	18.04 ± 4.14	41.15 ± 3.17	29.03 ± 2.14	47.98 ± 2.45
Dropwise with US	9.23 ± 2.26	23.12 ± 0.88	27.97 ± 1.24	48.56 ± 3.51

Table 4
Dissolution rate constant and R^2 obtained from the application of Higuchi model for recrystallized LASSBio-294.

Experiment	Higuchi	
	K_H	R^2
Raw LASSBio-294	9.6195	0.9074
Oven drying		
Quick without US	5.6132	**0.9991**
Quick with US	4.4359	**0.9980**
Dropwise without US	6.4720	**0.9967**
Dropwise with US	3.8677	**0.9984**
Spray drying		
Quick without US	5.5442	**0.9876**
Quick with US	6.5076	**0.9800**
Dropwise without US	5.1109	**0.9956**
Dropwise with US	5.2646	**0.9907**

conditions and difficulties of removal of the residual solvent from the crystal's structures. Finally, residual amounts of ionic liquid can change crystals morphologies.

Acknowledgments

The authors would like to thank Cristália Ltda (Itapira, São Paulo, Brazil) for providing the drug LASSBio-294 and CNPq (Brazilian National Research Council) for doctoral fellowship to Resende de Azevedo (Proc.200835/2010-6).

References

[1] H. Gonzalez-Serratos, R. Chang, E.F.R. Pereira, N.G. Castro, Y. Aracava, P.A. Melo, et al., A novel thienylhydrazone, (2-Thienylidene)3,4- methylenedioxybenzoylhydrazine, increases inotropism and decreases fatigue of skeletal muscle, J. Pharmacol. Exp. Ther. 299 (2001) 558–566.
[2] R.T. Sudo, G. Zapata-Sudo, E.J. Barreiro, The new compound, LASSBio 294, increases the contractility of intact and saponin-skinned cardiac muscle from Wistar rats, Br. J. Pharmacol. 134 (2001) 603–613, https://doi.org/10.1038/sj.bjp.0704291.
[3] J. Hecq, M. Deleers, D. Fanara, H. Vranckx, P. Boulanger, S. Lelamer, et al., Preparation and in vitro/in vivo evaluation of nano-sized crystals for dissolution rate enhancement of ucb-35440-3, a highly dosed poorly water-soluble weak base, Eur. J. Pharm. Biopharm. 64 (2006) 360–368, https://doi.org/10.1016/j.ejpb.2006.05.008.
[4] J.W. Mullin, Industrial Crystallization, Fourth edition, Butterwoth-Heinemann, 2001.
[5] Grodowska K, Parczewski A. Organic solvents in the pharmaceutical 2010:10.
[6] A. Forte, C.I. Melo, R. Bogel-Łukasik, E. Bogel-Łukasik, A favourable solubility of isoniazid, an antitubercular antibiotic drug, in alternative solvents, Fluid Phase Equilib. 318 (2012) 89–95, https://doi.org/10.1016/j.fluid.2012.01.022.
[7] G.S. Ha, J.-H. Kim, Effect of an ionic liquid on vancomycin crystallization, Korean J. Chem. Eng. 32 (2015) 576–582, https://doi.org/10.1007/s11814-015-0014-1.
[8] C. Lourenço, C.I. Melo, R. Bogel-Łukasik, E. Bogel-Łukasik, Solubility advantage of pyrazine-2-carboxamide: application of alternative solvents on the way to the future pharmaceutical development, J. Chem. Eng. Data 57 (2012) 1525–1533, https://doi.org/10.1021/je300044x.
[9] C.I. Melo, R. Bogel-Łukasik, M. Nunes da Ponte, E. Bogel-Łukasik, Ammonium ionic liquids as green solvents for drugs, Fluid Phase Equilib. 338 (2013) 209–216, https://doi.org/10.1016/j.fluid.2012.11.029.
[10] H. Mizuuchi, V. Jaitely, S. Murdan, A.T. Florence, Room temperature ionic liquids and their mixtures: Potential pharmaceutical solvents, Eur. J. Pharm. Sci. 33 (2008) 326–331, https://doi.org/10.1016/j.ejps.2008.01.002.
[11] K.B. Smith, R.H. Bridson, G.A. Leeke, Solubilities of pharmaceutical compounds in ionic liquids, J. Chem. Eng. Data 56 (2011) 2039–2043, https://doi.org/10.1021/je101040p.
[12] J. Resende de Azevedo, F. Espitalier, J.-J. Letourneau, M.I. Ré, Antisolvent crystallization of a cardiotonic drug in ionic liquids: Effect of mixing on the crystal properties, J. Cryst. Growth 472 (2017) 29–34, https://doi.org/10.1016/j.jcrysgro.2016.12.057.
[13] M.C. Kroon, V.A. Toussaint, A. Shariati, L.J. Florusse, J. van Spronsen, G.-J. Witkamp, et al., Crystallization of an organic compound from an ionic liquid using carbon dioxide as anti-solvent, Green Chem. 10 (2008) 333, https://doi.org/10.1039/b712848g.
[14] C.C. Weber, S.A. Kulkarni, A.J. Kunov-Kruse, R.D. Rogers, A.S. Myerson, The use of cooling crystallization in an ionic liquid system for the purification of pharmaceuticals, Cryst. Growth Des. 15 (2015) 4946–4951, https://doi.org/10.1021/acs.cgd.5b00855.
[15] A. Viçosa, J.-J. Letourneau, F. Espitalier, Ré M. Inês, An innovative antisolvent precipitation process as a promising technique to prepare ultrafine rifampicin particles, J. Cryst. Growth 342 (2012) 80–87, https://doi.org/10.1016/j.jcrysgro.2011.09.012.
[16] J.-H. An, J.-M. Kim, S.-M. Chang, W.-S. Kim, Application of ionic liquid to polymorphic design of pharmaceutical ingredients, Cryst. Growth Des. 10 (2010) 3044–3050, https://doi.org/10.1021/cg1001489.
[17] J.-H. An, W.-S. Kim, Antisolvent crystallization using ionic liquids as solvent and antisolvent for polymorphic design of active pharmaceutical ingredient, Cryst. Growth Des. 13 (2013) 31–39, https://doi.org/10.1021/cg300730w.
[18] J. Resende de Azevedo, J.-J. Letourneau, F. Espitalier, M.I. Ré, Solubility of a new cardioactive prototype drug in ionic liquids, J. Chem. Eng. Data 59 (2014) 1766–1773, https://doi.org/10.1021/je4009624.
[19] J. Resende de Azevedo, Etude de la cristallisation d'une nouvelle molécule à efficacité cardiotonique dans un mélange liquide ionique – eau, Univers. Toulouse (2014).
[20] F. Baillon, F. Espitalier, C. Cogné, R. Peczalski, O Louisnard, Crystallization and freezing processes assisted by power ultrasound, 2015.
[21] S.M. de la Parra-Arciniega, N.A. Garcia-Gomez, L.L. Garza-Tovar, D.I. García-Gutiérrez, E.M. Sánchez, Ultrasonic irradiation-assisted synthesis of Bi 2 S 3 nanoparticles in aqueous ionic liquid at ambient condition, Ultrason. Sonochem. 36 (2017) 95–100, https://doi.org/10.1016/j.ultsonch.2016.11.018.
[22] E. Kowsari, M. Mallakmohammadi, Ultrasound promoted synthesis of quinolines using basic ionic liquids in aqueous media as a green procedure, Ultrason. Sonochem. 18 (2011) 447–454, https://doi.org/10.1016/j.ultsonch.2010.07.020.
[23] G. Zbancioc, I.I. Mangalagiu, C. Moldoveanu, Ultrasound assisted synthesis of imidazolium salts: an efficient way to ionic liquids, Ultrason. Sonochem. 23 (2015) 376–384, https://doi.org/10.1016/j.ultsonch.2014.10.028.
[24] J.-Y. Zhang, Z.-G. Shen, J. Zhong, T.-T. Hu, J.-F. Chen, Z.-Q. Ma, et al., Preparation of amorphous cefuroxime axetil nanoparticles by controlled nanoprecipitation method without surfactants, Int. J. Pharm. 323 (2006) 153–160, https://doi.org/10.1016/j.ijpharm.2006.05.048.
[25] X.-S. Li, J.-X. Wang, Z.-G. Shen, P.-Y. Zhang, J.-F. Chen, J. Yun, Preparation of uniform prednisolone microcrystals by a controlled microprecipitation method, Int. J. Pharm. 342 (2007) 26–32, https://doi.org/10.1016/j.ijpharm.2007.04.025.
[26] P. Costa, J.M. Sousa Lobo, Modeling and comparison of dissolution profiles, Eur. J. Pharm. Sci. 13 (2001) 123–133.